20130726A

厚生労働科学研究費補助金

創薬基盤推進研究事業

# 認知症早期解析型マウスモデルの開発研究

平成２５年度　総括研究報告書

研究代表者　森　　啓

大阪市立大学・大学院医学研究科・教授

平成２６（２０１４）年　3月

厚生労働科学研究費補助金

創薬基盤推進研究事業

# 認知症早期解析型マウスモデルの開発研究

平成２５年度　総括研究報告書

研究代表者　森　　啓

大阪市立大学・大学院医学研究科・教授

平成２６（２０１４）年　3月

# 目　　次

# Ⅰ．総括研究報告

厚生労働科学研究費補助金（創薬基盤推進研究事業）
（総括）研究報告書

# 認知症早期解析型マウスモデルの開発研究に関する研究

研究代表者　森　啓　大阪市立大学・大学院医学研究科・教授

研究要旨
Aβオリゴマーはアルツハイマー病の発症原因として近年急速に注目されている分子種である。Aβオリゴマーの形成促進変異として発見された大阪変異を有するヒト APP 遺伝子を導入したトランスジェニックマウスを作製し、精査したところアルツハイマー病の初期変化である空間認知機能障害、LTP 異常、シナプス異常を認めた。しかしながら、アミロイド老人斑との関係も不明であり、神経原線維変化との関係も明らかではないことから、アルツハイマー病の脳病態の全過程を再現する上での意義を検証する事が大切である。この目的を達成するために、ヒトタウ遺伝子を発現するモデルマウスを作製し、両者の交配で得られるダブルトランスジェニックマウスを作製した。その結果、単独では神経原線維変化を形成しない正常型ヒトタウは、Aβオリゴマーによって、異常リン酸化されるだけではなく、神経原線維変化まで形成誘導されることが示された。以上の結果から、Aβオリゴマーは脳病態の中でも早期に作用し、後期病変であるタウ病変を誘導する事が示された。

研究分担者

富山　貴美　大阪市立大学大学院医学研究科・准教授

梅田　知宙　大阪市立大学大学院医学研究科・助教

## A．研究目的

アルツハイマー病（AD）の早期の段階であるpreclinicalあるいはprodromal stageを対象とするために、本研究では、初期変化と考えられている、Aβオリゴマーマウスと後期病態モデルと考えられているタウモデルを交配させたモデルマウスの解析を目的とする。

このことにより、早期病態変化としてのAβオリゴマーの意義が確立され、早期から晩期までの連続的な病態解明が可能となる。

## B．研究方法

後期病態モデルとしてヒトタウを発現するmini-genomic型タウを新たに作製し、大阪変異を発現するAβオリゴマーマウスの交配による新規モデルマウス作製を進める。

（1）ヒトタウを発現するmini-genomic型タウマウスは、CaMKinaseIIαプロモーターの下流に、ヒトタウ遺伝子の最長アイソフォームであるタウ441型cDNAに、イントロン9とイントロン10を導入したコンストラクトを構築した。エクソン10前後のイントロン構造は、＞10kbと長いことから、sｙプライシング供与配列、枝分かれ配列、受容の帰納演繹配列を保持するように工夫した。イントロン10には、FTDP-17変異であるA＋16Cを人工的に作製したものも同時に作製した。

これらの導入遺伝子コンストラクトを前核に微注入することでトランスジェニックマウスを作製した。

ヒトタウモデルマウスは、変異を持つもの、変異を持たないもの（2種類）が樹立することができたが、両モデルとも、アミノ酸変異はなく、全アミノ酸は野生型配列であり、孤発性疾患を代表したモデルと考えられる。

## C．研究結果

今回新規に作製したタウモデルマウスは、イントロン構造を有している事から、スプライシング可能かについて検討したところ、期待通りに正確なスプライシングを示すことが明らかとなった。さらに、エクソン10発現の有無によって、4リピートタウ、3リピートタウの２つのアイソフォームが産生される。生後の発達過程で、多くの動物では、3リピートタウから４リピートタウにスプライシ

ング変化することが知られているが、ヒトでは3リピートタウから3リピートタウ：4リピートタウが１：１になることが知られている。今回作製したタウモデルマウスでは、ヒトと同じく、幼若期で3リピートであるが、生後7,8週齢で１：１の混合型となっていることが確認された。この正常型ヒトタウモデルでは、学習能力、シナプス機能、脳病変のいずれにおいても24ヶ月齢まで異常を検出することができなかった。

導入遺伝子コンストラクト作製時に、FTDP-17変異の1つであるA＋16C変異をイントロン10に人為的に導入させた場合は、成熟後のヒトタウアイソフォームは、3リピートタウから、3リピートタウと4リピートタウの混合型となるが、両アイソフォーム比は、大きく4リピートに偏重し、タウは6ヶ月齢でLTP異常、異常リン酸化されていた。これタウの出現、空間認知機能障害の変化が生じ、12ヶ月齢でミクログリア反応、24ヶ月齢でニューロン死、アストログリア反応、神経原線維変化形成が生じることが観察され、ヒト脳内変化を再現していることが示された。

次に、Aβオリゴマーモデルと新規作製したヒトタウモデルの交配モデルを作製した。使用したヒトタウモデルは正常型タウモデルである。その理由は、正常型タウモデルもFTDP-17変異型タウモデルも、同じヒト野生型アミノ酸配列ではあるが、FTDP-17変異は、その変異自身で、病変を形成することから、Aβオリゴマーとの病態シグナル効果検証が難しくなると考えたからである。このようにして得られた同ブルトランスジェニックマウス（Aβオリゴマーｘ正常ヒトタウ）は、18ヶ月齢で、ニューロン死や神経原線維変化を形成することが見いだされた。ただし、24ヶ月例に至るまで、老人斑は形成されなかったことで、アミロイド老人斑の病態への関与が、いっそう希薄となったと言える。

## D．考察

Aβオリゴマーは、アルツハイマー病の早期病態変化であり、後期変化である神経原線維変化を誘導する上流に位置する。Aβオリゴマーは、マウスタウでは神経原線維変化を誘導せず、ヒトタウを必要とすることから、ヒトアミノ酸配列特異的なシグナルパスがあることが示唆された。このことは、治療戦略の時期選定という応用面からも重要な視点を与えている。すなわち、Aβオリゴマー、Aβオリゴマーからヒトタウへのシグナル伝搬、タウ病変の各々が、早期、中期、後期の治療薬対象であり、将来的には、患者各位のステージに沿った治療選択の指標となることが考察される。

今回のダブルトランスジェニックマウスの解析では、Aβオリゴマー自身の出現も単独のモデルでは８ヶ月例からの出現である処、６ヶ月例と明らかな早期出現されることが観察された。このことは、Aβオリゴマーとタウ病変は、完全な一方方向の病態シグナルであると考えるよりも、部分的な双方向性シグナルの可能性が考えられた。

## E．結論

アルツハイマー病の早期病態変化であり、特異的原因分子種であるAβオリゴマーは、正常型ヒトタウを神経原線維変化へと誘導する上流で作用する。

## F．健康危険情報

なし

## G．研究発表

### 1．論文発表


1）Kondo T, Asai M, Tsukita K, Kutoku Y, Ohsawa Y, Sunada Y, Imamura K, Egawa N, Yahata N, Okita K, Takahashi K, Asaka I, Aoi T, Watanabe A, Watanabe K, Kadoya C, Nakano R, Watanabe D, Maruyama K, Hori O, Hibino S, Choshi T, Nakahata T, Hioki H, Kaneko T, Naitoh M, Yoshikawa K, Yamawaki S, Suzuki S, Hata R, Ueno S, Seki T, Kobayashi K, Toda T, Murakami K, Irie K, Klein WL, Mori H, Asada T, Takahashi R, Iwata N, Yamanaka S, Inoue H. Modeling Alzheimer's disease with iPSCs reveals stress phenotypes associated with intracellular Aβ and differentialdrug responsiveness. **Cell Stem Cell.** 12:487-496 (2013)

2）Umeda T, Yamashita T, Kimura T, Ohnishi K, Takuma H, Ozeki T, Takashima5 A, Tomiyama T, Mori H. Neurodegenerative Disorder FTDP-17-Related Tau Intron 10 +16C→T Mutation Increases Tau Exon 10 Splicing and Causes Tauopathy in Transgenic Mice. **Am J Pathol.** 183:211-225 (2013)

3）Nomura S , Umeda T, Tomiyama T, Mori H. The E693D (Osaka) Mutation in Amyloid Precursor Protein Potentiates Cholesterol-Mediated Intracellular Amyloid b Toxicity Via Its Impaired Cholesterol Efflux. **J Neurosci Res.** 91:1541-1550 (2013)

4) Honjo Y, Horibe T, Torisawa A, Ito H, Nakanishi A, Mori H, Komiya T, Takahashi R, Kawakami K. Protein Disulfide Isomerase P5-Immunopositive Inclusions in Patients with Alzheimer's Disease. **J Alzheimers Dis.** 38:601-609 (2014)

5) Umeda T, Maekawa S, Kimura T, Takashima A, Tomiyama T, Mori H. Neurofibrillary tangle formation by introducing wild-type human tau into APP transgenic mice. **Acta Neuropathol.** 127:685-698 (2014)

**2. 学会発表**

1）森 啓
「日本における認知症医療の新展開：オレンジプランを踏まえて」
第23回 日本医療薬学会（宮城県仙台市）2013.9.21.

2）森 啓
「認知症医療の新展開：オレンジプラン施策考察」
第46回日本薬剤士会学術大会（大阪府大阪市）2013.9.22.

3）森 啓
「認知症の先進医療に必要な診断と戦略」
第３回日本認知症予防学会 （新潟県新潟市）2013.9.27.

4）森 啓
「脳神経外科医が支える認知症医療」
第72回日本脳神経外科学会学術総会（神奈川県横浜市）2013.10.16.

5）森 啓
「神経変性疾患における記憶障碍考」
第18回日本神経精神医学会（大阪府大阪市）2013.12.13.

6）森 啓
「認知症医療施策オレンジプラン2012について」
第７回日本薬局学会学術総会（大阪府大阪市）2013.11.24.

**H．知的財産権の出願・登録状況**
**（予定を含む。）**

**1. 特許出願・取得**
発明者：森啓・富山貴美・梅田知宙・森田隆・吉田佳世
発明の名称：ノックインマウス
出願番号：PCT/JP2014/53555
出願日：2014年2月14日

**2. 実用新案登録**
なし

**3.その他**
特になし

# II. 研究成果の刊行に関する一覧表

研究成果の刊行に関する一覧表

雑誌

| 発表者氏名 | 論文タイトル名 | 発表誌名 | 巻号 | ページ | 出版年 |
|---|---|---|---|---|---|
| Kondo T, Asai M, Tsukita K, Kutoku Y, Ohsawa Y, Sunada Y, Imamura K, Egawa N, Yahata N, Okita K, Takahashi K, Asaka I, Aoi T, Watanabe A, Watanabe K, Kadoya C, Nakano R, Watanabe D, Maruyama K, Hori O, Hibino S, Choshi T, Nakahata T, Hioki H, Kaneko T, Naitoh M, Yoshikawa K, Yamawaki S, Suzuki S, Hata R, Ueno S, Seki T, Kobayashi K, Toda T, Murakami K, Irie K, Klein WL, Mori H, Asada T, Takahashi R, Iwata N, Yamanaka S, Inoue H. | Modeling Alzheimer's disease with iPSCs reveals stress phenotypes associated with intracellular Aß and differentialdrug responsiveness. | Cell Stem Cell. | 12 | 487-496 | 2013 |
| Umeda T, Yamashita T, Kimura T, Ohnishi K, Takuma H, Ozeki T, Takashima5 A, Tomiyama T, Mori H. | Neurodegenerative Disorder FTDP-17-Related Tau Intron 10 +16C→T Mutation Increases Tau Exon 10 Splicing and Causes Tauopathy in Transgenic Mice. | Am J Pathol. | 183 | 211-222 | 2013 |
| Nomura S, Umeda T, Tomiyama T, Mori H. | The E693D (Osaka) Mutation in Amyloid Precursor Protein Potentiates Cholesterol-Mediated Intracellular Amyloid b Toxicity Via Its Impaired Cholesterol Efflux. | J Neurosci Res. | 91 | 1541-1550 | 2013 |
| Honjo Y, Horibe T, Torisawa A, Ito H, Nakanishi A, Mori H, Komiya T, Takahashi R, Kawakami K. | Protein Disulfide Isomerase P5-Immunopositive Inclusions in Patients with Alzheimer's Disease. | J Alzheimers Dis. | 38 | 601-609 | 2014 |
| Umeda T, Maekawa S, Kimura T, Takashima A, Tomiyama T, Mori H. | Neurofibrillary tangle formation by introducing wild-type human tau into APP transgenic mice. | Acta Neuropathol. | 127 | 685-698 | 2014 |

研究成果の刊行に関する一覧表

書籍

| 著者氏名 | 論文タイトル名 | 書籍全体の編集者名 | 書　籍　名 | 出版社名 | 出版地 | 出版年 | ページ |
|---|---|---|---|---|---|---|---|
| なし | | | | | | | |
| | | | | | | | |
| | | | | | | | |

# III. 研究成果の刊行物・別刷

Cell Stem Cell
Short Article

# Modeling Alzheimer's Disease with iPSCs Reveals Stress Phenotypes Associated with Intracellular Aβ and Differential Drug Responsiveness

Takayuki Kondo,[1,2,7] Masashi Asai,[7,9,10] Kayoko Tsukita,[1,7] Yumiko Kutoku,[11] Yutaka Ohsawa,[11] Yoshihide Sunada,[11] Keiko Imamura,[1] Naohiro Egawa,[1] Naoki Yahata,[1,7] Keisuke Okita,[1] Kazutoshi Takahashi,[1] Isao Asaka,[1] Takashi Aoi,[1] Akira Watanabe,[1] Kaori Watanabe,[7,10] Chie Kadoya,[7,10] Rie Nakano,[7,10] Dai Watanabe,[3] Kei Maruyama,[9] Osamu Hori,[12] Satoshi Hibino,[13] Tominari Choshi,[13] Tatsutoshi Nakahata,[1] Hiroyuki Hioki,[4] Takeshi Kaneko,[4] Motoko Naitoh,[5] Katsuhiro Yoshikawa,[5] Satoko Yamawaki,[5] Shigehiko Suzuki,[5] Ryuji Hata,[14] Shu-ichi Ueno,[15] Tsuneyoshi Seki,[16] Kazuhiro Kobayashi,[16] Tatsushi Toda,[16] Kazuma Murakami,[6] Kazuhiro Irie,[6] William L. Klein,[17] Hiroshi Mori,[18] Takashi Asada,[19] Ryosuke Takahashi,[2] Nobuhisa Iwata,[7,10,*] Shinya Yamanaka,[1,8] and Haruhisa Inoue[1,7,8,*]
[1]Center for iPS Cell Research and Application (CiRA)
[2]Department of Neurology, Graduate School of Medicine
[3]Department of Biological Sciences, Graduate School of Medicine and Department of Molecular and Systems Biology, Graduate School of Biostudies
[4]Department of Morphological Brain Science, Graduate School of Medicine
[5]Department of Plastic and Reconstructive Surgery, Graduate School of Medicine
[6]Organic Chemistry in Life Science, Division of Food Science and Biotechnology, Graduate School of Agriculture
Kyoto University, Kyoto 606-8507, Japan
[7]Core Research for Evolutional Science and Technology (CREST)
[8]Yamanaka iPS Cell Special Project
Japan Science and Technology Agency (JST), Saitama 332-0012, Japan
[9]Department of Pharmacology, Faculty of Medicine, Saitama Medical University, Saitama 350-0495, Japan
[10]Laboratory of Molecular Biology and Biotechnology, Department of Molecular Medicinal Sciences, Graduate School of Biomedical Sciences, Nagasaki University, Nagasaki 852-8521, Japan
[11]Department of Neurology, Kawasaki Medical School, Okayama 701-0192, Japan
[12]Department of Neuroanatomy (Biotargeting), Kanazawa University Graduate School of Medical Sciences, Ishikawa 920-8640, Japan
[13]Faculty of Pharmacy and Pharmaceutical Sciences, Fukuyama University, Hiroshima 729–0292, Japan
[14]Department of Functional Histology
[15]Department of Psychiatry
Ehime University Graduate School of Medicine, Ehime 791-0295, Japan
[16]Division of Neurology/Molecular Brain Science, Kobe University Graduate School of Medicine, Kobe, Hyogo 650-0017, Japan
[17]Department of Neurobiology, Northwestern University, Evanston, IL 60208, USA
[18]Department of Neuroscience, Graduate School of Medicine, Osaka City University, Osaka 545-8585, Japan
[19]Department of Neuropsychiatry, Institute of Clinical Medicine, University of Tsukuba, Ibaraki 305-8577, Japan
*Correspondence: haruhisa@cira.kyoto-u.ac.jp (H.I.), iwata-n@nagasaki-u.ac.jp (N.I.)
http://dx.doi.org/10.1016/j.stem.2013.01.009

## SUMMARY

Oligomeric forms of amyloid-β peptide (Aβ) are thought to play a pivotal role in the pathogenesis of Alzheimer's disease (AD), but the mechanism involved is still unclear. Here, we generated induced pluripotent stem cells (iPSCs) from familial and sporadic AD patients and differentiated them into neural cells. Aβ oligomers accumulated in iPSC-derived neurons and astrocytes in cells from patients with a familial amyloid precursor protein (APP)-E693Δ mutation and sporadic AD, leading to endoplasmic reticulum (ER) and oxidative stress. The accumulated Aβ oligomers were not proteolytically resistant, and docosahexaenoic acid (DHA) treatment alleviated the stress responses in the AD neural cells. Differential manifestation of ER stress and DHA responsiveness may help explain variable clinical results obtained with the use of DHA treatment and suggests that DHA may in fact be effective for a subset of patients. It also illustrates how patient-specific iPSCs can be useful for analyzing AD pathogenesis and evaluating drugs.

## INTRODUCTION

Alzheimer's disease (AD) is the most prevalent neurodegenerative disorder. One of the pathological features of AD is the oligomerization and aggregation and accumulation of amyloid-β peptide (Aβ), forming amyloid plaques in the brain. Cognitive impairment observed in clinical AD is inversely well correlated with the amount of Aβ oligomers in the soluble fraction rather than the amount of Aβ fibrils (amyloid plaques) constituting the oligomers (Haass and Selkoe, 2007; Krafft and Klein, 2010). Increasing evidence has shown that Aβ oligomers extracted from AD model mice or made from synthetic peptides cause

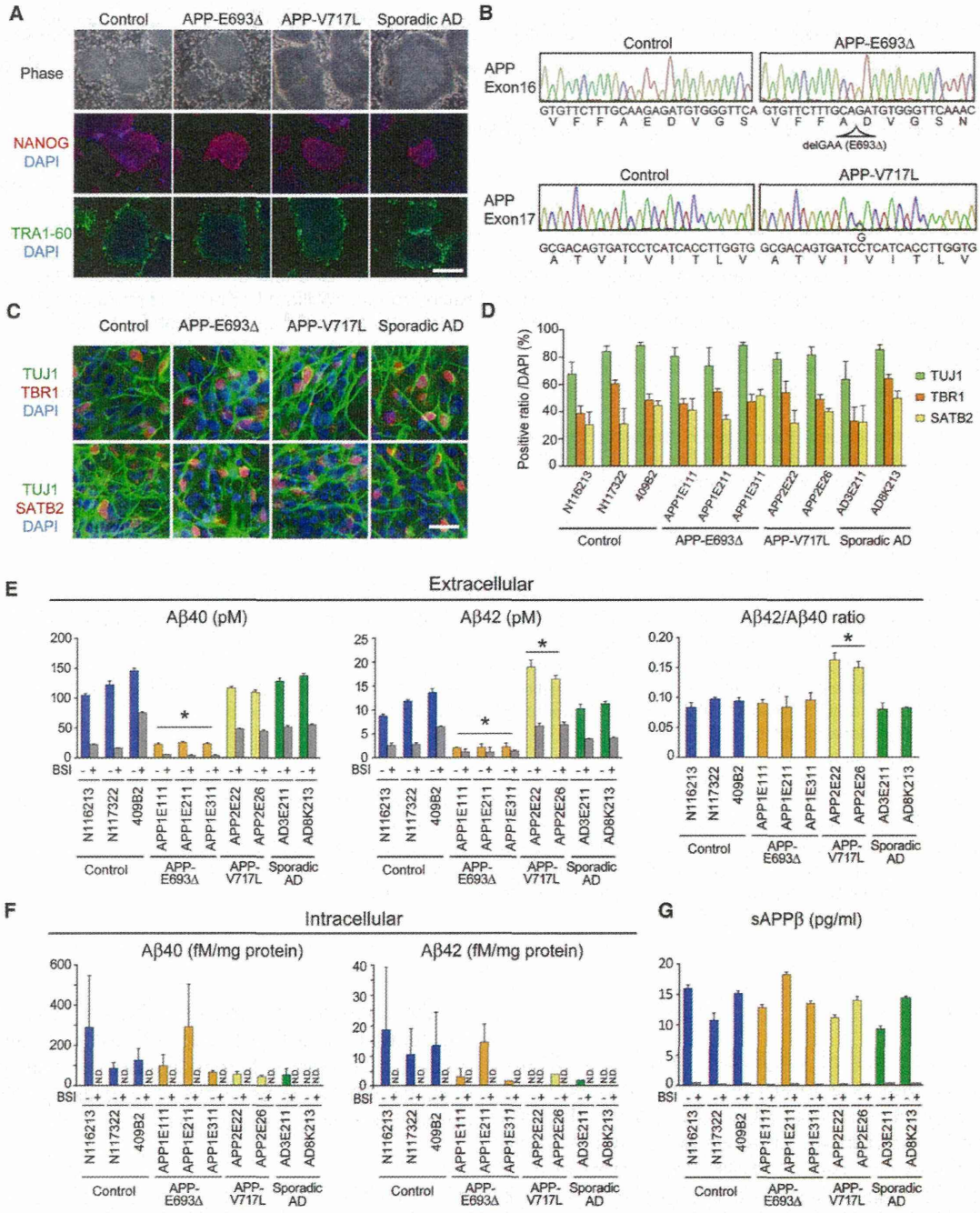


**Figure 1. Establishment of Control and AD Patient-Specific iPSCs, and Derivation of Cortical Neurons Producing Aβs from iPSCs**

(A) Established iPSCs from both controls and AD patients showed embryonic stem cell-like morphology (Phase) and expressed pluripotent stem cell markers NANOG (red) and TRA1-60 (green). The scale bar represents 200 μm.

(B) Genomic DNA sequences showed the presence of the homozygous genotype for E693 deletion and the heterozygous genotype for V717L mutation on the *APP* gene only in AD iPSCs.

(C) Estimation of neuronal differentiation from control and AD-iPSCs. After 2 months of differentiation, neurons were immunostained with antibodies against the neuronal marker TUJ1 and the cortical neuron markers TBR1 and SATB2. The scale bar represents 30 μm.

(D) Proportions of TUJ1-, TBR1-, and SATB2-positive cells in control and AD-iPSCs. Data represent mean ± SD (n = 3 per clone).

(E) Aβ40 and Aβ42 secreted from iPSC-derived neural cells into the medium (extracellular Aβ) were measured at 48 hr after the last medium change. Data represent mean ± SD (n = 3 per clone). Levels of Aβ40 and Aβ42 in AD(APP-E693Δ) without β-secretase inhibitor IV (BSI, 1 μM) were significantly lower than those of the others (*, $p < 0.006$), and the level of Aβ42 and the ratio of Aβ42/Aβ40 in AD(APP-V717L) without BSI were significantly higher than those of the others

*(legend continued on next page)*

neurotoxicity and cognitive impairments in vitro and in vivo (Walsh et al., 2002; Gong et al., 2003; Lesné et al., 2006), and this was also true in humans (Kuo et al., 1996; Shankar et al., 2008; Noguchi et al., 2009). Therefore, the formation and accumulation of Aβ oligomers has been presumed to play a central role in the pathogenesis and clinical symptoms of AD. Aβs are composed of 38–43 amino acid residues and are generated from the amyloid precursor protein (APP) by β- and γ-secretase-mediated sequential cleavages. A number of mutations linked to familial AD in the *APP* gene have been identified. Recently, an atypical early-onset familial AD, caused by an E693Δ mutation of an APP-producing variant Aβ lacking 22$^{nd}$ Glu was discovered in Japan (Tomiyama et al., 2008). This APP-E693Δ mutation presents rare, autosomal-recessive mutations of the *APP* gene related to familial AD. Patients with the mutation show overt early-onset symptoms of AD but lack Aβ deposition, according to positron emission tomography (PET) scan analysis with a [$^{11}$C] Pittsburgh compound-B (PIB) radioprobe (Tomiyama et al., 2008; Shimada et al., 2011). The 22$^{nd}$ Glu within the Aβ sequence has a destabilizing effect on the formation of oligomeric structures because of the electrostatic repulsion between the adjacent side chain of 22$^{nd}$ Glu (Kassler et al., 2010), and the deletion of the amino acid residue leads to the ready formation of Aβ oligomers in vitro (Nishitsuji et al., 2009). APP-E693Δ transgenic mice show AD-like pathology, including intracellular oligomer accumulation, but lack extracellular amyloid plaque formation (Tomiyama et al., 2010). However, it remains unclear whether Aβ oligomers are accumulated in familial and sporadic AD patient neural cells and how intracellular Aβ oligomers play a pathological role. The compound and/or drugs that might rescue the Aβ oligomer-induced pathological phenotypes are also unclear. Recent developments in induced pluripotent stem cell (iPSC) technology have facilitated the investigation of phenotypes of patient neural cells in vitro and have helped to overcome the lack of success in modeling sporadic AD.

Here, we report the derivation and neuronal and astroglial differentiation of iPSCs from a familial AD patient with an APP-E693Δ mutation, a familial case with another APP mutation, as well as other sporadic cases. Using patient neurons and astrocytes, we addressed the accumulation and possible pathological roles of intracellular Aβ oligomers in familial and sporadic AD. We found that Aβ oligomers were not proteolytically resistant and that docosahexaenoic acid (DHA) treatment attenuated cellular phenotypes of AD neural cells with intracellular Aβ oligomers in both familial and sporadic AD patients.

## RESULTS

### iPSC Generation and Cortical-Neuronal Differentiation

Dermal fibroblasts were reprogrammed by episomal vectors (Okita et al., 2011). Control iPSC lines from three unrelated individuals, three and two familial AD iPSC lines from patients with E693Δ[AD(APP-E693Δ)] and V717L[AD(APP-V717L)] APP mutations, respectively, and two sporadic iPSC lines (AD3E211 and AD8K213) from two unrelated patients (Figure S1A available online) were generated (Figures 1A, 1B, and S1B–S1H). To characterize cortical neurons derived from the iPSC lines, we established differentiation methods for cortical neurons by modifying previous procedures (Morizane et al., 2011) (Figure S1I). The differentiated cells expressed the cortical neuron subtype markers SATB2 and TBR1 (Figure 1C), and the differentiated neurons were functionally active (Figures S1J and S1K). There was no prominent difference in the differentiation propensity between control and AD neurons (Figures 1D and S1L).

We analyzed the amounts of extra- and intracellular Aβ40 and Aβ42 (Figures 1E and 1F). As expected, both Aβ species were strongly decreased in all cloned AD(APP-E693Δ) neural cells in comparison to those in control neural cells. In familial AD(APP-V717L) neural cells, an increase in the extracellular Aβ42 level and a corresponding decrease in the intracellular Aβ42 level were observed, and the Aβ42/Aβ40 ratio in the culture medium was increased up to 1.5-fold, suggesting that the abnormality of APP metabolism in AD is dependent on the mutation sites in *APP*. Extracellular Aβ levels in sporadic AD neural cells were not changed in comparison to those in control neural cells, but intracellular Aβ in sporadic AD8K213 neural cells apparently decreased (that is, below the detection limit). APP expression levels in the AD(APP-E693Δ) neural cells were lower than in the others, but the levels of α- and β-secretase-mediated APP processing remained unaltered in all neural cells (Figures 1G, S1M, and S1N). Soluble APPβ production was strongly inhibited by treatment with β-secretase inhibitor IV (BSI) (Figure 1G). Aβ levels in the original fibroblasts and iPSC-derived astrocytes, in which APP expression levels were relatively higher than those in neural cells (data not shown), were lower than those of the corresponding neural cells (Figures S1O and S1P).

### Intracellular Accumulation of Aβ Oligomers in AD(APP-E693Δ) and in One of the Sporadic AD Neural Cells

Using an immunocytochemical method with the Aβ-oligomer-specific antibody NU1 (Lambert et al., 2007), we investigated whether AD(APP-E693Δ) neural cells harbor Aβ oligomers or not. We found that Aβ oligomers were accumulated as puncta in the neurons of AD(APP-E693Δ) and in one of the sporadic AD cases (Figure 2A). The area of Aβ-oligomer-positive puncta was significantly increased in AD(APP-E693Δ) neuronal cells relative to control neuronal cells (Figure 2B). Dot blot analysis using cell lysates revealed that Aβ oligomers were markedly elevated in the AD(APP-E693Δ) and sporadic AD8K213 neural cells (Figures 2C and 2D), whereas Aβ oligomers were not detected in the culture medium (data not shown). Another antibody against Aβ, 11A1, which detects low-molecular-weight oligomers rather than the Aβ monomer (Murakami et al., 2010), showed results similar to those observed with NU1 (Figures

(*, $p < 0.001$). There are significant differences between dimethyl sulfoxide (DMSO)-control and BSI treatment in each case (*, $p < 0.001$) except that of AD(APP-E693Δ) for Aβ42.

(F) Aβ40 and Aβ42 in cell lysates (intracellular Aβ). N.D., not detected. Data represent mean ± SD (n = 3 per clone).

(G) The amount of soluble APPβ was not altered in control and AD. Data represent mean ± SD (n = 3 per clone).

See also Figure S1.

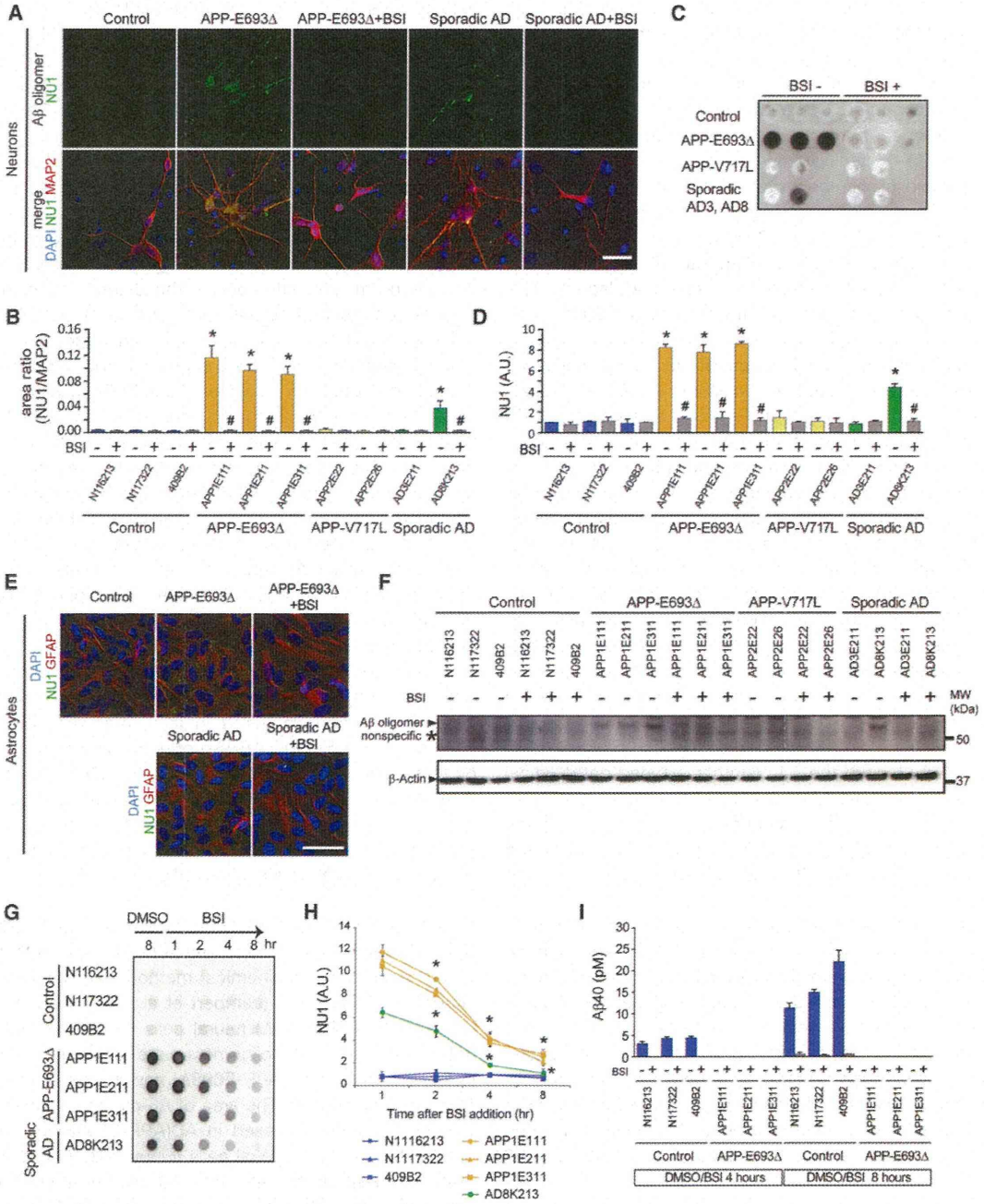


**Figure 2. Familial AD(APP-E693Δ) and Sporadic AD iPSC-Derived Neurons Have Intracellular Aβ Oligomers**

(A) Intracellular Aβ oligomer accumulation in iPSC-derived neurons (red, MAP2-positive cells) was detected by the Aβ-oligomer-specific monoclonal antibody NU1 (green) with a punctate pattern. Aβ oligomer accumulation was massive in AD(APP-E693Δ) and sporadic AD(AD8K213) neurons but only faint in control neurons. Treatment with 1 μM BSI decreased Aβ oligomer accumulation. DAPI, nuclear staining (blue). The scale bar represents 30 μm.

(B) Quantification of Aβ oligomer accumulation in (A); the ratio of the NU1-positive area in the MAP2-positive area was analyzed. Data represent mean ± SD (n = 3 per clone). Aβ oligomer levels in the AD(APP-E693Δ) and sporadic AD(AD8K213) neural cells without BSI were significantly different from those of other neural cells (*, $p < 0.005$) and from corresponding neural cells with BSI (#, $p < 0.005$).

(C) Dot blot analysis with the use of NU1 antibody. Control (N116213, N117322, 409B2), APP-E693Δ(APP1E111, APP1E211, APP1E211), APP-V717L (APP2E22, APP2E26), and sporadic AD (AD3E211, AD8K213) neural cells were dotted from the left. Blank is RIPA buffer only.

(D) Signals of blot in (C) were quantified. Data represent mean ± SD (n = 3 per clone). Aβ oligomer levels in AD(APP-E693Δ) and sporadic AD(AD8K213) neurons without BSI were significantly different from those of other neurons (*, $p < 0.001$) and from corresponding neurons treated with 1 μM BSI (#, $p < 0.001$).

(E) Aβ oligomer accumulation in AD astrocytes. The scale bar represents 30 μm.

*(legend continued on next page)*

S2A–S2D). However, Aβ oligomers were not detected in cell lysates from the fibroblasts that generate iPSC lines (Figure S2E). To confirm whether Aβ oligomers were derived from mutant APP(E693Δ), we transduced a lentiviral vector driven by an EF1α promoter to overexpress wild or mutant APP(E693Δ) in control iPSC-derived neural cells and found that Aβ oligomers emerged inside control neural cells overexpressing mutant APP(E693Δ) (Figure S2F).

To investigate the intracellular accumulation of Aβ oligomers in astrocytes derived from control and AD iPSCs, we established an astrocyte-enrichment culture by modifying the method previously reported (Krencik et al., 2011) (Figures S2G–S2J). Dot blot analysis using Aβ oligomer antibodies revealed that the astrocytes of AD(APP-E693Δ) and one of the sporadic AD iPSCs accumulated Aβ oligomers intracellularly (Figures 2E, S2K, and S2L), which was compatible with the results of neurons. On the other hand, we detected no difference in the uptake of extracellular glutamate between control and AD astrocytes (Figure S2M).

Aβ oligomers were also detected as a protein band with a molecular mass of 50~60 kDa by western blot analysis (Figures 2F and S2N). The accumulation of Aβ oligomers was inhibited by treatment with BSI (Figures 2A–2G, S2A–S2D, and S2N). To clarify whether the E693Δ mutation results in accelerated Aβ oligomerization and/or in a proteolytically resistant and stable form of Aβ oligomers, we analyzed the levels of Aβ oligomers over a course of time after BSI treatment. Intracellular Aβ oligomers started to disappear from 2 hr after the treatment with BSI, almost reaching the control level by 8 hr (Figures 2G and 2H). Secretion of Aβ40 from control neural cells was already inhibited at 2 hr after BSI treatment, but the secretion from AD neural cells was under the detection limit in both the presence and absence of BSI (Figure 2I).

## Cellular Stress Responses Caused By Intracellular Aβ Oligomers in AD iPSC-Derived Neural Cells

Extracellular Aβ deposition in patient brains carrying APP with an E693Δ mutation is predicted to be extremely low, as amyloid PET imaging with a [$^{11}$C] PIB probe revealed a far lower signal in the patients than those observed in sporadic AD brains (Tomiyama et al., 2008). Given that processing by β- and γ-secretases largely proceeds within vesicular endosomal compartments, it was possible that Aβ oligomers were associated with specific organelles. We characterized the Aβ oligomer-positive punctate structures in AD(APP-E693Δ) neural cells and astrocytes by coimmunostaining with antibodies for markers of vesicular compartments and subcellular organelles. Subpopulations of Aβ oligomer-positive puncta in the AD neurons showed positive immunostaining for an endoplasmic reticulum (ER) marker, binding immunoglobulin protein (BiP); an early endosomal marker, early endosome-associated antigen-1 (EEA1); and a lysosomal marker, lysosomal-associated marker protein 2 (LAMP2) (data not shown).

To uncover molecules that might be implicated in the dysfunction of AD(APP-E693Δ) neural cells, we analyzed gene expression profiles of control and AD neural cells (Figure 3A and Table S1). Gene ontology analysis revealed that oxidative-stress-related categories, including peroxiredoxin, oxidoreductase, and peroxidase activities, were upregulated in the AD, whereas glycosylation-related categories were downregulated (Figures 3B and 3C and Table S1), suggesting that ER and Golgi function might be perturbed in AD neural cells. Western blot analysis clarified that the amounts of both BiP and cleaved caspase-4 were elevated in the neurons and astrocytes of the AD(APP-E693Δ) case, and that of BiP in one of the sporadic AD cases, AD8K213, but not in fibroblasts (Figures 3D–3F and S3A–S3F). We also found that BSI treatment not only prevented the increase in Aβ oligomer-positive puncta area per cell in the context of AD(APP-E693Δ) lines but also decreased the amount of BiP and cleaved caspase-4 (Figures 3D–3F). *PRDX4*-coding antioxidant protein peroxiredoxin-4 was the most highly upregulated gene (Figure 3C). Western blot analysis confirmed that the amount of peroxiredoxin-4 was increased up to approximately 5- to 7-fold in lysates from AD(APP-E693Δ) and in one of the sporadic AD cases, AD8K213 neural cells, but not in fibroblasts, and was decreased by the BSI treatment (Figures 3D, 3G, S3A, S3D, S3G, and S3H), indicating that the antioxidant stress response was provoked by Aβ oligomer formation in AD(APP-E693Δ) and sporadic AD8K213. To identify pathogenic species evoking oxidative stress in AD(APP-E693Δ), we visualized reactive oxygen species (ROS) and found that ROS was increased in both neurons and astrocytes in AD(APP-E693Δ) and AD8K213 (Figures 3H–3J and S3I –S3L). This increase was counteracted by the BSI treatment. These results indicated that intracellular Aβ oligomers provoked both ER and oxidative stress, and the increase in ROS most likely occurred via a vicious cycle between ER and oxidative stress (Malhotra and Kaufman, 2007).

## Alleviation of Intracellular Aβ Oligomer-Induced Cellular Stress by DHA

We evaluated BSI and three additional drugs that had been reported to improve ER stress or to inhibit ROS generation: (1) DHA (Begum et al., 2012), (2) dibenzoylmethane (DBM14-26) (Takano et al., 2007), and (3) NSC23766 (Lee et al., 2002) (Figures 4 and S4). DHA treatment significantly decreased the protein level of BiP, cleaved caspase-4, and peroxiredoxin-4 in AD (APP-E693Δ) neural cells (Figures 4A, 4B, S4A, and S4B), and BiP and peroxiredoxin-4 in sporadic AD8K213 (Figures S4C and S4D). Furthermore, DHA treatment also decreased the generation of ROS in AD(APP-E693Δ) neural cells (Figures 4C and 4D), whereas the amount of Aβ oligomers in cell lysates

(F) Western blot analysis of control and AD neural cells in the presence or absence of BSI. BSI treatment (1 μM) disappeared 6E10-positive ≈55 kDa protein bands in cell lysates of AD(APP-E693Δ) and sporadic AD(AD8K213) neural cells.

(G) Disappearance of Aβ oligomers after BSI treatment was analyzed by dot blot analysis with the use of the NU1 antibody. Intracellular Aβ oligomers started to disappear 2 hr after BSI treatment.

(H) Signals of blots in (G) were quantified. Data represent mean ± SD (n = 3 per clone). BSI treatment (1 μM) decreased intracellular Aβ in AD neural cells and was reduced to 16~23% of vehicle control by 8 hr. Post hoc analysis revealed that the amounts of Aβ oligomers at 2 hr after BSI treatment were significantly decreased in comparison to those of DMSO control oligomers (*, $p < 0.005$).

(I) Changes in extracellular Aβ40 levels were analyzed in the experimental condition of (G). Data represent mean ± SD (n = 3 per clone).

See also Figure S2.

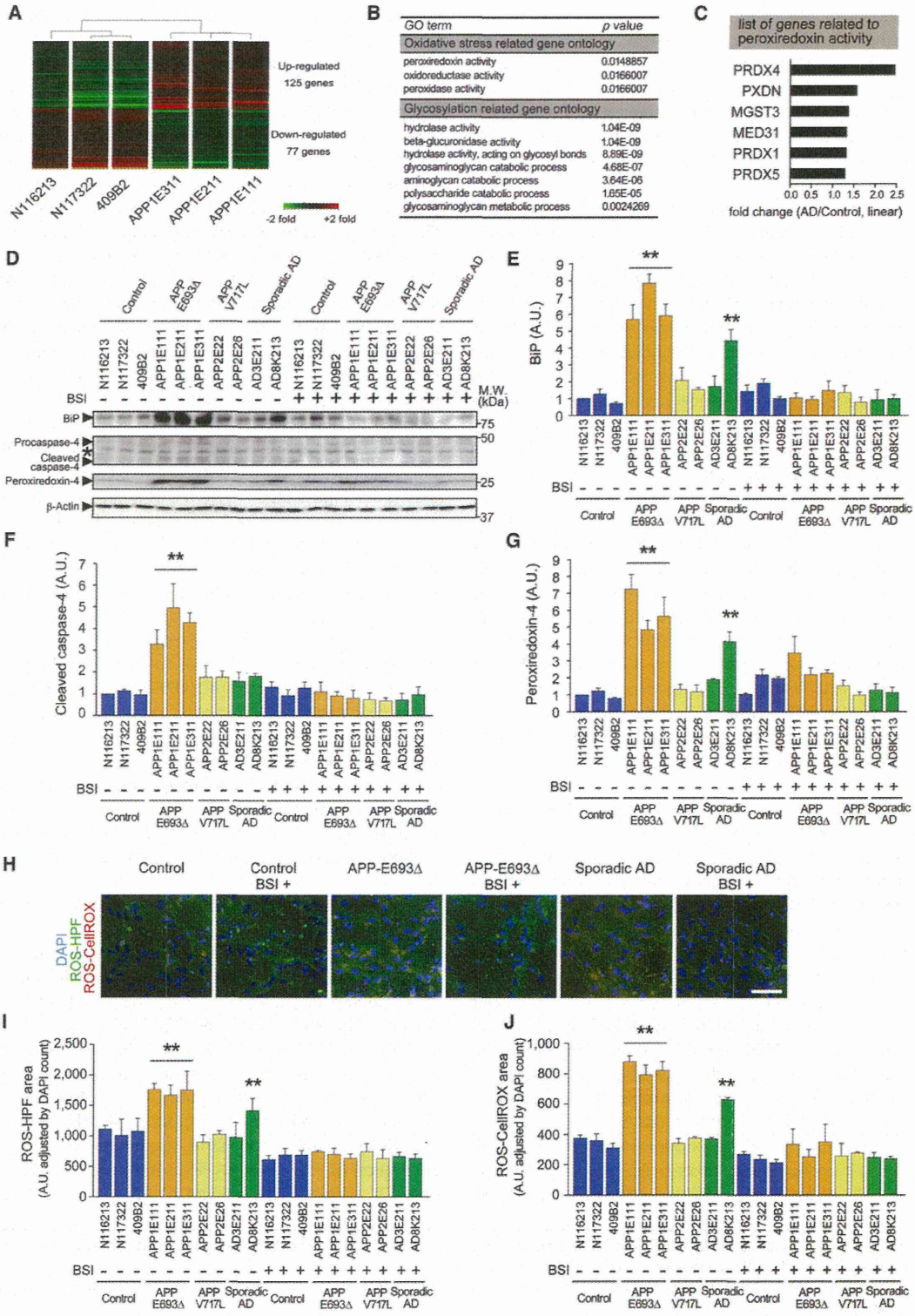


**Figure 3. Cellular Stress Responses Caused by Intracellular Aβ Oligomers in Familial AD(APP-E693Δ) and Sporadic AD(AD8K213) iPSC-Derived Neural Cells**

(A) Hierarchical clustering analysis of differentiated neuronal cells and a heatmap of significantly up- and downregulated genes in AD neural cells. The statistically significant cutoff p value is < 0.05.

*(legend continued on next page)*

was not altered (Figures S4E–S4G). In contrast, the high concentration of DHA, DBM14-26, or NSC23766 treatment increased the protein level of BiP (Figure S4B). Finally, to confirm the protective effects of DHA in short-term screening, we analyzed the effect on the survival of AD(APP-E693Δ) neural cells. Neuronal cells were labeled with a lentiviral vector expressing synapsin I-promoter-driven EGFP and cultivated in the medium depleted of neurotrophic factors and neural culture supplements mix. The real-time survival rate of AD(APP-E693Δ) neurons was lower than that of normal control neurons; however, DHA treatment for 16 days partially rescued AD(APP-E693Δ) cell viability (Figures 4E–4G). The real-time survival rate of sporadic AD(AD3E211, AD8K213) neurons for 16 days was unchanged (Figures 4E and 4F and Table S2). We confirmed these results through a lactate dehydrogenase (LDH) assay (Figure 4G). The AD(APP-E693Δ) neurons were also vulnerable to oxidative stress by hydrogen peroxide treatment (Figure S4H). Extracellular Aβ levels were not altered in the assay (Figure 4H).

## DISCUSSION

The present study shows that neural cells derived from a patient carrying the pathogenic APP-E693Δ mutation and a sporadic AD patient produce intracellular Aβ oligomers, and the use of these neural cells provided an experimental system for addressing whether such oligomers would cause cellular stress and the killing of neurons and how such intracellular Aβ oligomers might contribute to the disease pathogenesis, despite only one patient carrying the E693Δ mutation being available. Our findings also suggest that the possible heterogeneity of familial and sporadic AD stems from phenotypic differences of intracellular Aβ oligomers and suggests the possibility that DHA, a drug that failed in some clinical trials of AD treatment, might be effective in a portion of AD patients.

We demonstrated that Aβ oligomers were formed and accumulated inside AD(APP-E693Δ) and sporadic AD(AD8K213) neurons by immunostaining (Figures 2A and 2B), dot blot analysis (Figures 2C and 2D), and western blot analysis (Figures 2F and S2N). In addition, intracellular accumulation of Aβ oligomers, which has been supposed to be proteolytically resistant, disappeared after treatment with BSI in both AD neurons (Figures 2G and 2H), indicating that AD(APP-E693Δ) and sporadic AD(AD8K213) neurons still seemed to retain a degrading activity toward Aβ oligomers in which proteasomes, autophagosomes, and/or lysosomes may be involved and, thereby, that the pathological property of Aβ oligomers in a part of AD might be completely abrogated. The sporadic AD(AD8K213) neurons may retain a specific cellular environment that permits the formation of Aβ oligomers. Additional studies aimed at identifying the factors causing such an environment are needed.

We observed that the accumulation of Aβ oligomers induced ER and oxidative stress both in AD(APP-E693Δ) and in sporadic AD(AD8K213) neurons, although caspase-4 activation appeared not to accompany sporadic AD, probably because of the lesser extent of ER stress in comparison to AD(APP-E693Δ). Previously, Nishitsuji et al. (2009) reported that accumulated Aβ oligomers in ER provoke ER stress. This result suggests that oligomers represent a self-aggregating state of Aβ. During this process, Aβ generates ROS, which is supported by the fact that Aβ coordinates the metal ions zinc, iron, and copper, which induce the oligomerization of Aβ. Iron and copper then cause the generation of toxic ROS and calcium dysregulation (Barnham et al., 2004), leading to membrane lipid peroxidation and the impairment of the function of a range of membrane-associated proteins (Hensley et al., 1994; Butterfield, 2003), antioxidant factors being thought to protect ER-stress-induced cellular toxicities (Malhotra and Kaufman, 2007).

We found that intracellular Aβ oligomers were accumulated not only in a case of familial AD with APP-E693Δ mutation but also in a sporadic AD case, although only three clones derived from one familial AD patient carrying an APP-E693Δ mutation and two clones from two sporadic AD patients were analyzed in this study because of the limited number of patients. In contrast, in familial AD with the APP-V717L mutation, of which only one case was available, intracellular Aβ oligomers were not detected, but the extracellular Aβ42/Aβ40 ratio, which is increased in mutant presenilin-mediated familial AD, as reported previously (Yagi et al., 2011), was increased, lending support to the notion that AD could be classified into two categories: extracellular Aβ type and intracellular Aβ type. Although it has been supposed that environmental factors and/or the aging process contribute to neurodegenerative diseases, our findings support the idea that a genetic factor might play a role in a part of sporadic AD, a finding that is compatible with a previous report (Israel et al., 2012). However, identifying the genetic factor would require a larger sample size. The sporadic AD case with intracellular Aβ oligomers might correspond to the case without extracellular Aβ40 elevation of Israel et al. (2012). Analysis of neurons

(B) The gene ontology (GO) term list, calculated from the significantly altered gene expression patterns in the microarray analysis of AD versus control neural cells.
(C) Altered expression levels of genes related to peroxidation activity detected by GO analysis. All values were significantly different from that of the control ($p < 0.05$).
(D–G) Western blot analysis of ER stress markers (BiP and casapase-4), peroxiredoxin-4, and a reference protein (β-actin) in the presence or absence of BSI. (E–G) Densitometric analysis of (D) are shown. Measured values of proteins were normalized by β-actin. Data represent mean ± SD (n = 3 per clone). Levels of BiP (E), cleaved caspase-4 (F), and peroxiredoxin-4 (G) in AD(APP-E693Δ) and sporadic AD(AD8K213) neural cells without BSI were significantly different from those of the other neural cells (**, $p < 0.005$).
(H) Typical images of reactive oxygen species (ROS) staining, detected by HPF or CellROX, in control and AD neural cells with or without BSI treatment. Scale bars represent 30 μm.
(I and J) Quantitative data of (H), ROS-HPF (I), and ROS-CellROX (J). Each value was shown as a ratio of the HPF-stained or CellROX area (average of random 25 fields per sample) adjusted with DAPI counts. Data represent mean ± SD (n = 3 per clone). ROS-generation levels in AD(APP-E693Δ) and sporadic AD(AD8K213) neural cells were significantly different from those of the others (**, $p < 0.001$). Data represent mean ± SD (n = 3 per clone).
See also Figure S3 and Table S1.

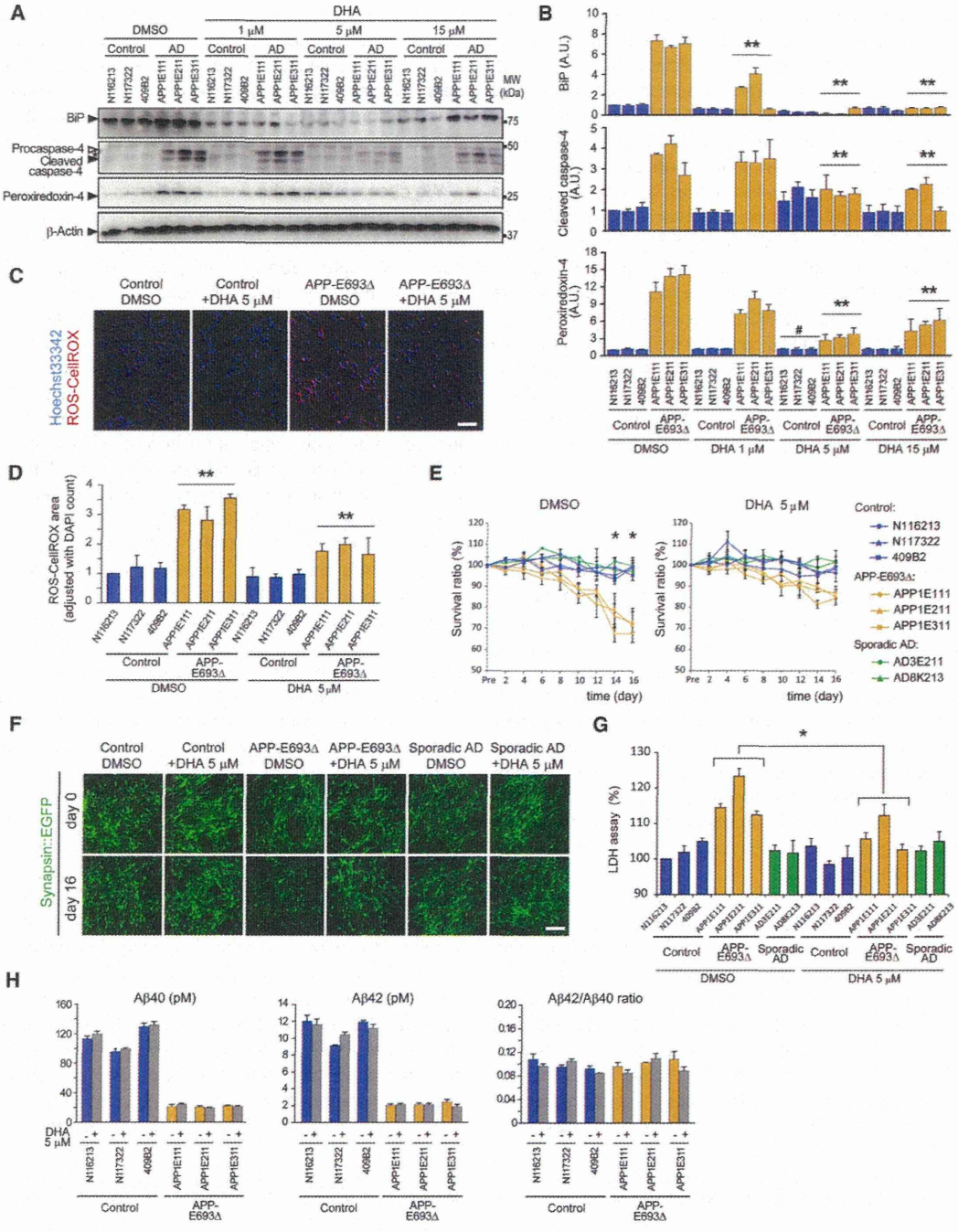


**Figure 4. DHA-Alleviated Cellular Stress Caused By Intracellular Aβ Oligomers**

(A) Control and AD(APP-E693Δ) neural cells at day 72 were treated with DHA for 48 hr. Then, cells were lysed and subjected to immunoblot analysis (1 μM, 5 μM, and 15 μM of docosahexaenoic acid [DHA]).

(B) Densitometric analysis of (A) is shown. Measured values were normalized by that of β-actin. Data represent mean ± SD (n = 3 per clone). Two-way analysis of variance (ANOVA) showed significant main effects of DHA treatment (BIP, $F_{[3,64]} = 136.712$, $p < 0.001$; cleaved caspase-4, $F_{[3,64]} = 50.855$, $p < 0.001$) with a significant interaction between APP mutation and DHA treatment (BIP, $F_{[3,64]} = 99.658$, $p < 0.001$; cleaved caspase-4, $F_{[3,64]} = 53.005$, $p < 0.001$). Post hoc analysis revealed significant differences between DMSO (control) and DHA treatment (1, 5, and 15 μM) in AD(APP-E693Δ) neural cells (**, $p < 0.001$). Two-way ANOVA for peroxiredoxin-4 showed significant main effects of DHA treatment ($F_{[3,64]} = 16.995$; $p < 0.001$) with a significant interaction between APP mutation and DHA treatment ($F_{[3,64]} = 32.093$; $p < 0.001$). Post hoc analysis revealed significant differences between DMSO-control and DHA treatment (5 and 15 μM) in AD(APP-E693Δ) neural cells (**, $p < 0.001$). In control neural cells, the 5 μM DHA group was significantly different from the other groups (#, $p < 0.005$).

(C) Typical images of ROS-CellROX and Hoechst33342 signals after treatment with vehicle or 5 μM DHA. The scale bar represents 50 μm.

*(legend continued on next page)*

and astrocytes, as we performed here, from larger numbers of patients might result in the classification of sporadic AD.

To date, the clinical effectiveness of DHA treatment is still controversial (Freund-Levi et al., 2006; Quinn et al., 2010). It is of particular interest that one of two sporadic AD neurons accumulated intracellular Aβ oligomers and showed cellular phenotypes that could respond to DHA but the other did not, and this result may explain why DHA treatment was effective for some AD patients, those with the intracellular Aβ oligomer-associated type of AD, although the timing (that is, the stage of disease development) for starting the treatment would be another critical factor. These results may suggest that patient-specific iPSCs provide a chance to re-evaluate the effect of a drug that failed in AD clinical trials, depending on the selection of the patient type. In the present study, the amount of Aβ oligomers in our culture was not affected by DHA, although it would be effective for reducing cellular stresses, and reducing the oligomerization of Aβ was also presumed to be a candidate mechanism of DHA treatment (Cole and Frautschy, 2006). These results indicate that therapy with DHA would alleviate symptoms. Furthermore, the data showing that BSI treatment leads to a reduction in ROS formation at a relatively similar level (Figure 2G) in both AD and control cells might indicate an Aβ oligomer-independent effect, in addition to an Aβ oligomer-dependent effect, of BSI.

In any event, patient-specific iPSCs would provide disease pathogenesis, irrespective of the disease being in a familial or sporadic form, as well as enable the evaluation of drug and patient classification of AD.

## EXPERIMENTAL PROCEDURES

### Derivation of Patient-Specific Fibroblasts

Control and AD-derived human dermal fibroblasts (HDFs) were generated from explants of 3 mm dermal biopsies. After 1–2 weeks, fibroblast outgrowths from the explants were passaged.

### iPSC Generation

Human complementary DNAs for reprogramming factors were transduced in HDFs with episomal vectors (*SOX2, KLF4, OCT4, L-MYC, LIN28*, and small hairpin RNA for p53). Several days after transduction, fibroblasts were harvested and replated on an SNL feeder cell layer. On the following day, the medium was changed to a primate embryonic stem cell medium (ReproCELL, Japan) supplemented with 4 ng/ml basic FGF (Wako Pure Chemicals Industries, Japan). The medium was changed every other day. iPSC colonies were picked up 30 days after transduction.

### Statistical Analysis

All data are shown as mean ± SD. For comparisons of the mean between two groups, statistical analysis was performed by applying Student's t tests after confirming equality between the variances of the groups. When the variances were unequal, Mann-Whitney U tests were performed (SigmaPlot 11.2.0, Systat Software, USA). Comparisons of the mean among three groups or more were performed by one-way, two-way, or three-way analysis of variance followed by a post hoc test with the use of Student-Newman-Keuls Method (SigmaPlot 11.2.0). p values < 0.05 were considered significant.

## ACCESSION NUMBERS

The Gene Expression Omnibus accession numbers for microarray data reported in this paper are GSE43326 (gene-expression comparison between control and AD clones), GSE43382 (gene-expression change along with the astroglial differentiation), and GSE43328 (gene-expression comparison of generated iPSCs).

## SUPPLEMENTAL INFORMATION

Supplemental Information contains Supplemental Experimental Procedures, four figures, and two tables and can be found with this article online at http://dx.doi.org/10.1016/j.stem.2013.01.009.

## ACKNOWLEDGMENTS

We would like to express our sincere gratitude to all our coworkers and collaborators, Mari Ohnuki, Megumi Kumazaki, Mitsuyo Kawada, Fumihiko Adachi, Takako Enami, and Misato Funayama for technical assistance; Nobuya Inagaki and Norio Harada for technical advice; and Kazumi Murai for editing the manuscript. This research was funded in part by a grant from the Funding Program for World-Leading Innovative R&D on Science and Technology (FIRST Program) of the Japan Society for the Promotion of Science (JSPS) to S.Y., from the Alzheimer's Association (IIRG-09-132098) to H.M., from the JST Yamanaka iPS Cell Special Project to S.Y. and H.I., from CREST to H.I., H.M., N.I., and T.T., from a Grant-in-Aid from the Ministry of Health, Labour and Welfare of Japan to H.I., from a Grant-in-Aid for Scientific Research on Innovative Area "Foundation of Synapse and Neurocircuit Pathology" (22110007) from the Ministry of Education, Culture, Sports, Science and Technology of Japan to H.I. and N.I., and from the Japan Research Foundation for Clinical Pharmacology to H.I. H.I. conceived the project; T.K., N.I., M.A., and H.I. designed the experiments; T.K., N.I., M.A., K.W., C.K., R.N., N.E., N.Y. and K. Tsukita performed the experiments; T.K., N.I., M.A., and H.I. analyzed the data; K.O., I.A., K.M., T.N., K.I., W.L.K., O.H., S.H., and T.C. contributed

(D) Quantitative data of (C) is shown. Each value indicated the ratio of the CellROX-stained area (an average of random 25 fields per sample) adjusted with DAPI counts. Data represent mean ± SD (n = 3 per clone). Two-way ANOVA showed significant main effects of DHA treatment ($F_{[1,32]} = 43.140$; $p < 0.001$) with a significant interaction between the APP mutation and DHA treatment ($F_{[3,32]} = 23.410$; $p < 0.001$). The DHA group in AD(APP-E693Δ) neural cells was significantly different from the other groups (**, $p < 0.005$).

(E) Real-time survival rate of control and AD neural cells with and without DHA showing cell viability. The numbers of control and AD(APP-E693Δ) neurons with Synapsin I-promoter-driven EGFP were sequentially imaged (average of 25 random fields per sample) and counted to assess the survival ratio (n = 3 per clone). Data represent mean ± SD (n = 3 per clone). In the cell-survival ratio, three-way ANOVA showed significant main effects of the APP mutation ($F_{[1,256]} = 377.611$; $p < 0.001$), DHA treatment ($F_{[1,256]} = 36.117$; $p < 0.001$), and time ($F_{[7,256]} = 65.272$; $p < 0.001$), with significant interactions between the APP mutation and DHA treatment ($F_{[1,256]} = 18.315$; $p < 0.001$), between the APP mutation and time ($F_{[7,256]} = 20.023$; $p < 0.001$), between DHA treatment and time ($F_{[7,256]} = 4.534$; $p < 0.001$), and among all three factors ($F_{[7,256]} = 5.277$; $p < 0.001$). Post hoc analysis revealed that, on day 14 and day 16, AD(APP-E693Δ) neural cells were more vulnerable in the long culture than control neural cells and that DHA treatment rescued the vulnerability (*, $p < 0.001$).

(F) Typical images of Synapsin::EGFP neurons used in real-time survival assay. The scale bar represents 50 μm.

(G) Cytotoxicity in neural culture derived from control and AD iPSCs after treatment with DHA (5 μM) for 16 days. Measured fluorescent lactate dehydrogenase (LDH) release served as a measure of cytotoxicity. Data represent mean ± SD (n = 3 per clone). Two-way ANOVA showed significant main effects of DHA treatment ($F_{[1,32]} = 16.710$; $p < 0.001$) with a significant interaction between APP-E693Δ mutation and DHA treatment ($F_{[3,32]} = 9.210$; $p < 0.005$). There was a significant difference in AD(APP-E693Δ) neural cells between the DMSO-control and DHA groups (*, $p < 0.05$).

(H) Aβ40 and Aβ42 secreted from iPSC-derived neurons into medium (extracellular Aβ) at day 16 of the long-term culture were measured at 48 hr after the last medium change. Data represent mean ± SD (n = 3 per clone).

See also Figure S4 and Table S2.